# Quantitative Conformational Study of Redox-Active [2]Rotaxanes, Part 1: Methodology and Application to a Model [2]Rotaxane

## Silvano Altobello, Kirill Nikitin,* Jacek K. Stolarczyk,* Elena Lestini, and Donald Fitzmaurice[a]

**Abstract:** This paper reports a novel methodology for the conformational analysis of [2]rotaxanes. It combines NMR spectroscopic (COSY, NOESY and the recently reported paramagnetic line-broadening and suppression technique) and electrochemical techniques to enable a quantitative analysis of the co-conformations of interlocked molecules and the conformations of their components. This methodology was used to study a model [2]rotaxane in solution. This [2]rotaxane consists of an axle that incorporates an electron-poor, doubly positively charged violo-gen that threads an electron-rich crown ether. It has been shown that the axle of the [2]rotaxane in its dicationic state adopts a folded conformation in solution and the crown ether is localised at the viologen moiety. Following a one-electron reduction of viologen, the paramagnetic radical cation of the [2]rotaxane retains its folded conformation in solution. The data also demonstrate that in the radical cation the crown ether remains localised at the viologen, despite its reduced affinity for the singly reduced viologen. The combined quantitative NMR spectroscopic and electrochemical characterisation of the electromechanical function of the model [2]rotaxane in solution provides an important reference point for the study of switching in structurally related bistable [2]rotaxanes, which is the subject of the second part of this work.

**Keywords:** cyclic voltammetry · molecular modeling · radical ions · rotaxanes · supramolecular chemistry

## Introduction

Interlocked molecules, such as rotaxanes and catenanes, have been intensively studied owing to a large number of potential applications in molecular electronic devices.[1] In particular, these systems may exist in several diastereoisomeric structural forms,[2] which are usually referred to as translational isomers or co-conformations.[3] Application of an external stimulus, such as a change in pH,[4] a change of electric potential[5] or photochemical excitation,[6] can induce interconversion of the co-conformations of the rotaxanes or catenanes by shuttling or circumrotational motions of the components of the systems, respectively.[1,5,7] Hence, these molecules may function as controllable molecular-level switches or mechanical devices.

Electrochemical and photochemical switching of bistable [2]rotaxanes has been known for more than a decade.[5,6,8] In general, [2]rotaxanes comprise a dumbbell-shaped component (hereafter referred to as an axle), which can include one or more recognition sites (stations) and a ring component. A representation of a simple viologen-based [2]rotaxane that contains only one electron-deficient, electrochemically active viologen station and one electron-rich crown ether ring is shown in Figure 1. In such redox-active molecules the position of the crown ether along the axle is thought to be predominantly determined by the electrochemical states of the stations.[5] Therefore, a change in the
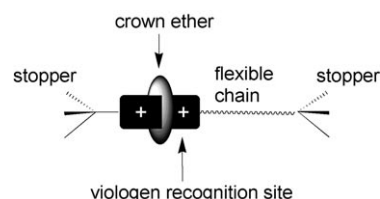
[a] S. Altobello, Dr. K. Nikitin, Dr. J. K. Stolarczyk, E. Lestini, Prof. D. Fitzmaurice
School of Chemistry and Chemical Biology
University College Dublin
Belfield, Dublin 4 (Ireland)
Fax: (+353) 1-716-2127
E-mail: kirill.nikitin@ucd.ie
jacek.stolarczyk@ucd.ie

Supporting information for this article is available on the WWW under http://www.chemeurj.org/ or from the author.

Figure 1. Schematic representation of a model [2]rotaxane.

electrochemical state of these stations may induce an interconversion between the co-conformations of the molecule. However, despite great progress in the studies of the interconversion process in rotaxanes and catenanes,[1,3,5,7,9] relatively little is known about the conformations of the individual components of the system in various oxidation states; this particularly relates to paramagnetic states for which the application of NMR spectroscopy is usually problematic.[3b] The lack of full understanding of these interlocked molecular systems hinders the progress in developing their applications because their function often relies on the components being in a particular conformation. It is clear that there is a need for a general approach for the determination of the co-conformations and conformations in various oxidation states and to understand the relationship between conformation and function.

For example, in a recent paper we described the self-assembly and electrochemical switching of a heterosupramolecular system that consisted of a tripodal bistable [2]rotaxane adsorbed at the surface of a titanium dioxide nanoparticle.[10] Our findings appeared to suggest that electron transfer and shuttling were accompanied by significant conformational changes of the components, which included folding of the axle. The study also raised important questions regarding the strength of the interactions between the crown ether and viologen stations in different oxidation states. On one hand, it showed that there was still a measurable interaction between them after the first, and even the second, electron reduction of the viologen moiety. On the other hand, we later found that a [2]pseudorotaxane that consisted of a similar viologen moiety dissociated after the first electron reduction, which indicated a very weak interaction in the reduced state.[11] Such seemingly inconsistent results provide further arguments for a more rigorous approach to the conformational analysis of the [2]rotaxanes in different oxidation states.

In this paper we report a novel methodology to quantitatively study the diastereoisomerism and conformations of rotaxanes in solution. To date, several NMR spectroscopy techniques, particularly COSY and NOESY,[12] have proven to be very useful in sensitive and non-invasive structure characterisation of [2]rotaxanes and catenanes.[13] The NMR spectroscopy techniques were used together with cyclic voltammetry (CV),[1c] mass spectrometry[13e] or continuous-wave EPR spectroscopy.[7g] 2D-IR spectroscopy was used to observe the changes in the co-conformations on a picosecond timescale.[7h] Although application of NMR spectroscopy to paramagnetic species (such as a singly reduced viologen-based rotaxane) is limited, it has recently been demonstrated that important structural information may be obtained by a quantitative analysis of paramagnetic line-broadening and suppression (PASSY) in [2]rotaxanes.[11] Herein, we combine the results of NOESY data with PASSY, electrochemical and reference crystallographic data. The combined results are compared by using the concept of effective distances with a number of hypothetical diastereoisomers obtained by molecular mechanics modelling with different

spatial constraints. This procedure enabled us to identify the structure that most closely matches the experimental data.

The application of the NOE technique relies on the ability to resolve and assign the relevant resonances in the NMR spectrum. This assignment proved to be very difficult for the bistable [2]rotaxane system described earlier.[10] The spectrum of that system also contains a number of peaks that are irrelevant for the conformational analysis of [2]rotaxanes. For these reasons and for clarity, herein the methodology is applied to a less complicated model redox-active [2]rotaxane (Figure 1). The [2]rotaxane consists of an axle that incorporates a single electron-poor viologen station and threads an electron-rich crown ether. It was envisaged that such a design would retain the basic interaction between the components of analogous bistable [2]rotaxanes and significantly simplify the structure to permit unambiguous full assignment of all of the signals observed in the NMR spectra in the aromatic and aliphatic regions. It is important that such a simplification does not compromise the ability to study the role of folding of the flexible chain in the axle in detail and to study the interaction between the viologen station and the crown ether.

Accordingly, the conformation of the model [2]rotaxane ($8·2PF_6$) in its parent dication state and single-electron reduced state ($8^··2PF_6$) was quantitatively characterised in solution by using NOE and PASSY NMR spectroscopy techniques. The results were supplemented by the electrochemical characterisation of $8·2PF_6$ and also by the molecular mechanics modelling of its two hypothetical diastereoisomers. The reported findings support the notion that the electromechanical function of the redox-active model [2]rotaxane depends not only on the affinities of the components of the interlocked molecule for each other in different oxidation states, but also on the conformations of the components.

This paper describes the synthesis of $8·2PF_6$, the conformational analysis of the dication state of $8·2PF_6$ in solution, followed by the conformational analysis of the singly reduced [2]rotaxane $8^··PF_6$ and a discussion of the electrochemical data. Details of the assignment of NMR spectra are given in the Supporting Information.

Further investigations of switching in two-station [2]rotaxanes by using the methodology presented herein are reported in detail in the second part of this work.[11b]

## Results and Discussion

**Synthesis of the model [2]rotaxane**: Model [2]rotaxane $8·2PF_6$ (Scheme 1) has been designed so that the first bulky stopper group ($S_A$) is rigidly attached to the viologen moiety ($V$) at one of the nitrogen atoms. The other nitrogen of $V$ is connected through a flexible polyether linker chain to the second bulky stopper ($S_B$). These stoppers ensure that the molecular axle $9·2PF_6$ remains interlocked with crown ether $7$.

The synthesis of the $S_A$–$V$ component of $5·PF_6$ is shown in Scheme 2. Initially, tris-(4-*tert*-butylphenyl)methanol (**2**) was
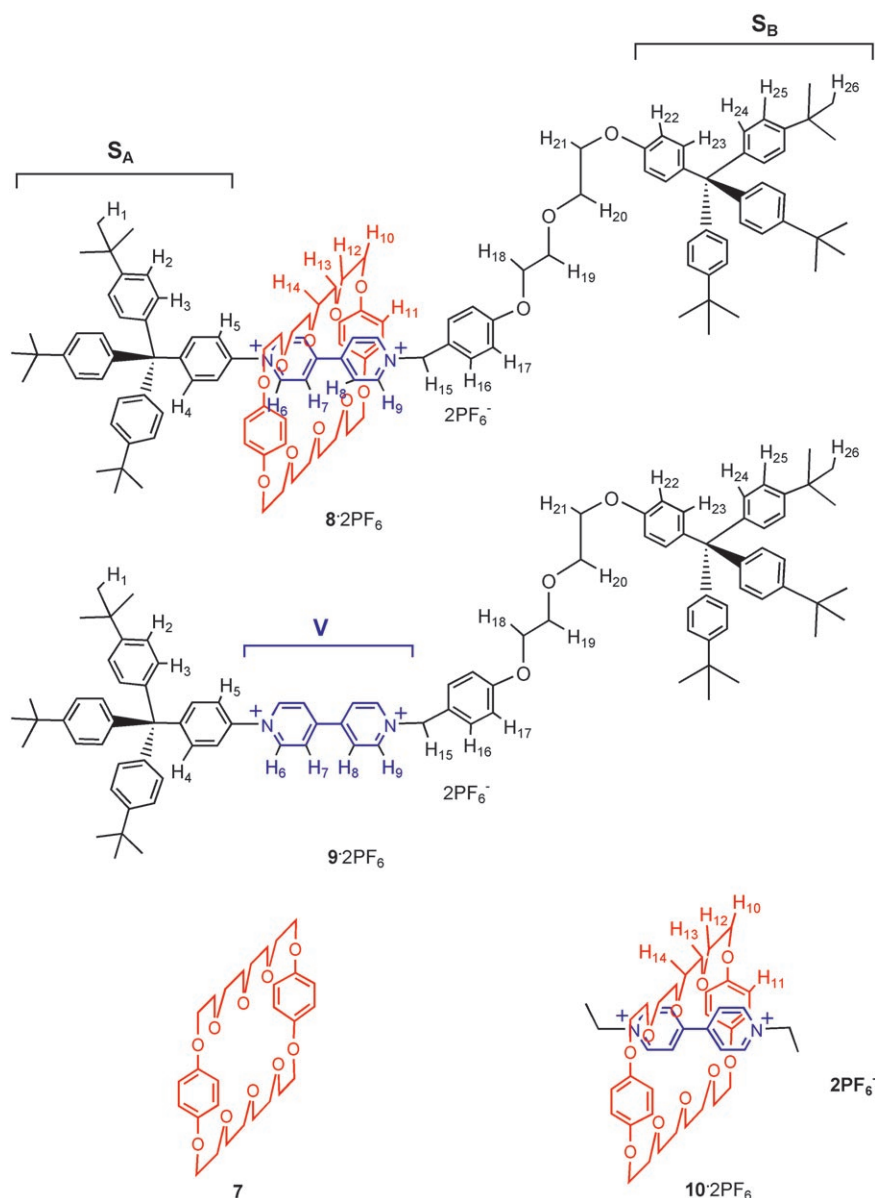
Scheme 1. Chemical structures **8**·2PF$_6$ and related components. The numbering corresponds to the NMR spectrum shown in Figure 2.
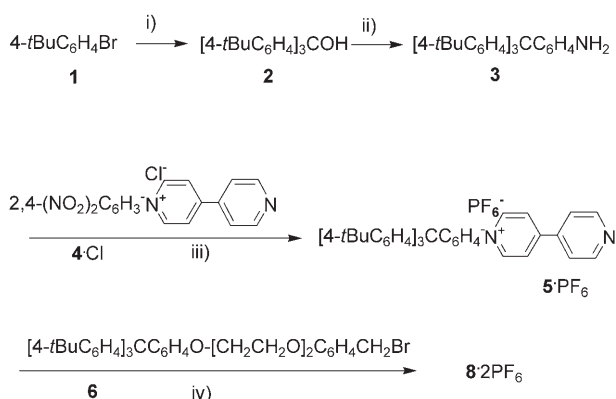


Scheme 2. Synthesis of **8**·2PF$_6$. Reagents and conditions: i) 1) BuLi; 2) Et$_2$CO$_3$, 0 °C, THF, 12 h;[15] ii) PhNH$_3$Cl, acetic acid, 100 °C, 24 h, 93 %; iii) EtOH; reflux; 24 h; 73 %; iv) 7, benzonitrile, 5 d, RT, 56 %.

prepared from 1-bromo-4-*tert*-butylbenzene (**1**) and diethyl carbonate in a yield of 56 %. Alcohol **2** was converted into the corresponding aniline (**3**) by using a previously reported procedure,[14a] which involved an electrophilic aromatic substitution in acetic acid with an excess of aniline hydrochloride as the substrate. Chloride **5**·Cl was obtained by the nucleophilic reaction of **3** with 1-(2,4-dinitrophenyl)-4,4′-bipyridinium chloride (**4**·Cl).[14b] Chloride **5**·Cl was purified by column chromatography and converted into the corresponding hexafluorophosphate (**5**·PF$_6$).[14a]

Substrate **5**·PF$_6$ was alkylated with flexible stopper component **6** in the presence of **7**. Applying our recently reported high-concentration approach to the synthesis of [2]rotaxanes at room temperature and atmospheric pressure,[15c] [2]rotaxane **8**·2PF$_6$ was obtained in a good yield (56 %).

Owing to the fact that our attempts to crystallise **8**·2PF$_6$ were unsuccessful, a structurally related [2]pseudorotaxane (**10**·2PF$_6$, Scheme 1) was prepared and fully characterised by X-ray crystallography.

[2]Rotaxane **8**·2PF$_6$ gave the well-resolved $^1$H NMR spectrum shown in Figure 2. It was possible, therefore, to make a full and unambiguous assignment of all of the proton resonances in this spectrum (Table S1 in the Supporting Information). These assignments were made by using standard COSY and 1D NOE data, which are also given in the Supporting Information.

**Structural NMR study of 8·2PF$_6$ in solution**: A quantitative NOE study of **8**·2PF$_6$ was used to estimate the interatomic distances in solution. The NOE measurements were obtained from a double pulsed field gradient spin echo (DPFGSE-NOE) experiment in deoxygenated acetonitrile at 25 °C.

The NOE spectrum of **8**·2PF$_6$ was recorded when the crown ether aromatic protons (H$_{11}$) were irradiated at $\delta =$ 6.14 (Figure S6 in the Supporting Information). All NOE enhancements were positive, which demonstrated relatively
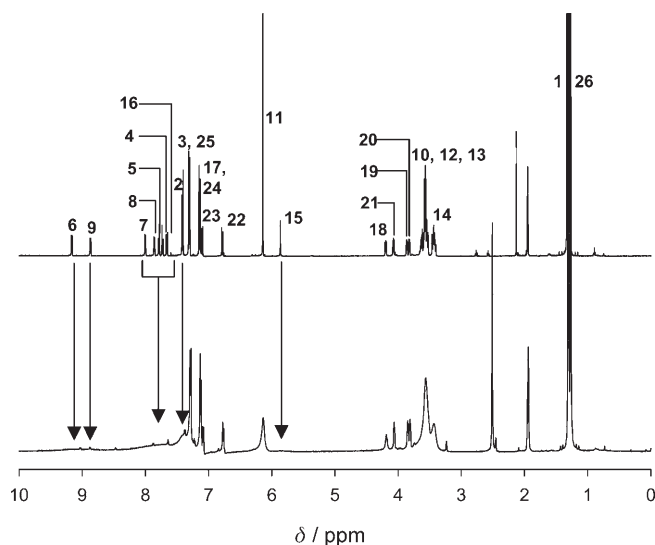
Figure 2. $^1$H NMR of $\mathbf{8}\cdot2\,\mathrm{PF_6}$ (top) and its radical cation $\mathbf{8}\cdot\mathrm{PF_6}$ (bottom). Numbering is in accordance with that shown in Scheme 1.

fast tumbling of the molecule under the conditions reported. The intensities of the observed NOE enhancements were interpreted on the basis of the assumption that the contributions of molecular motion and spin diffusion were equal for all positions in the molecule.[12]

The calculations of interatomic distances in $\mathbf{8}\cdot2\,\mathrm{PF_6}$ in solution were done by using crystallographic data for [2]pseudorotaxane $\mathbf{10}\cdot2\,\mathrm{PF_6}$ as a reference. Specifically, the distances between protons $H_{11}$ and $H_{10}$ in the crystal structure of $\mathbf{10}\cdot2\,\mathrm{PF_6}$ (Figure 3) were used to obtain the reference dis-
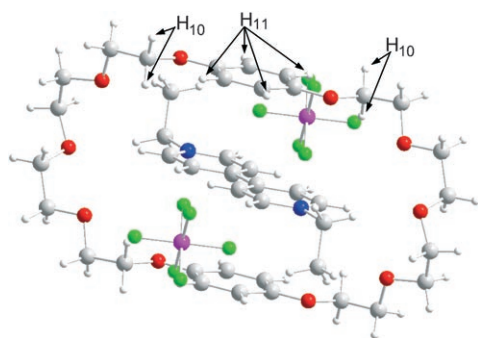


Figure 3. The crystal structure of $\mathbf{10}\cdot2\,\mathrm{PF_6}$.

tance ($d_{\mathrm{ref}}$). This value for $d_{\mathrm{ref}}$ corresponds to an imaginary experiment in which the NOE signal of $H_{10}$ is measured when the $H_{11}$ protons of $\mathbf{10}\cdot2\,\mathrm{PF_6}$ are irradiated. Whereas $\mathbf{10}\cdot2\,\mathrm{PF_6}$ is, at first glance, much simpler than $\mathbf{8}\cdot2\,\mathrm{PF_6}$, the viologen moieties in both structures are almost identical and they incorporate the same crown ether ($\mathbf{7}$). Therefore, it is expected that the average distances between protons $H_{11}$ and $H_{10}$ of $\mathbf{7}$ would be similar is both cases.

Generally, using solid-state data to elucidate the structure in solution can only be considered an approximation owing to the crystal lattice packing and solvation effects.[16,17] In

this case, it may be expected that $d_{\mathrm{ref}}$ in the solid state is slightly shorter than the distances between protons $H_{11}$ and $H_{10}$ in the solution structures of both $\mathbf{8}\cdot2\,\mathrm{PF_6}$ and $\mathbf{10}\cdot2\,\mathrm{PF_6}$ because there is the possibility that rotation about the C–O bonds will move the adjacent methylene groups out of the aromatic plane.

The value of 3.20 Å for $d_{\mathrm{ref}}$ was obtained according to Equation (1):

$$d_{\mathrm{ref}} = \left( \frac{1}{N_{\mathrm{ref}}} \sum_{i}^{n_{\mathrm{ir}}} \sum_{j}^{n_{\mathrm{ref}}} d_{\mathrm{ij}}^{-6} \right)^{-1/6} \tag{1}$$

in which $n_{\mathrm{ir}}$ ($=8$) is the number of irradiated $H_{11}$ protons, $n_{\mathrm{ref}}$ ($=8$) is the number of reference $H_{10}$ protons. Hence, $N_{\mathrm{ref}} = n_{\mathrm{ref}}n_{\mathrm{ir}}$ is the number of interacting irradiated–reference pairs in the system. The values of $d_{\mathrm{ij}}$ are the distances between protons $H_{11}$ and $H_{10}$, which were obtained from the X-ray crystallographic data of $\mathbf{10}\cdot2\,\mathrm{PF_6}$.

Employing the value obtained above for $d_{\mathrm{ref}}$, the effective distances between sets of chemically equivalent protons $H_{11}$ and $H_x$ in $\mathbf{8}\cdot2\,\mathrm{PF_6}$ were evaluated by using Equation (2). Here, the effective distance ($d_x$) denotes the average distance in terms of the NOE interaction (sixth power decay with distance).

$$d_x = d_{\mathrm{ref}} \left( \frac{N_{\mathrm{ref}}}{N_x} \times \frac{\mathrm{NOE}_x}{\mathrm{NOE}_{\mathrm{ref}}} \right)^{-1/6} \tag{2}$$

$\mathrm{NOE}_x$ is the cross-peak volume integral for the set of equivalent protons ($H_x$) of interest, which was extracted from the NOE spectrum of $\mathbf{8}\cdot2\,\mathrm{PF_6}$. These volumes are given in Table S2 in the Supporting Information. $N_x$ is the corresponding number of interacting proton–proton pairs, which is equal to $n_{\mathrm{ir}}n_x$ in which $n_x$ is the number of $H_x$ protons in the analysed set. $\mathrm{NOE}_{\mathrm{ref}}$ is the cross-peak volume integral for protons $H_{10}$.[18]

Analysis of the effective proton–proton distances estimated from the NOE spectrum (Table 1) is particularly useful for $\mathbf{V}$ protons $H_6$ to $H_9$. For instance, the effective $d_6$ and $d_9$ distances are almost identical (4.35 and 4.31 Å, respectively), which is also the case for distances $d_7$ and $d_8$ (3.86 and 3.85 Å, respectively). These results show that $\mathbf{7}$ is localised at $\mathbf{V}$. Furthermore, these results agree well with the distances observed in the crystal structure of $\mathbf{10}\cdot2\,\mathrm{PF_6}$ (Figure 3).

Interestingly, the estimated distance from protons $H_{11}$ to protons $H_{16}$ in $\mathbf{7}$ ($d_{16} = 4.20$ Å) is shorter than the distance to the $H_9$ protons ($d_9 = 4.31$ Å). This finding may be explained in terms of the tilt of the $N$-benzyl aromatic ring with respect to the plane of $\mathbf{V}$. The tilt arises from the sp$^3$ hybridisation of the $N$-benzyl methylene carbon and causes the $H_{16}$ protons to be lifted above the plane of $\mathbf{V}$ and approach the crown ether aromatic protons. For similar reasons, the effective distance ($d_5 = 4.41$ Å) of the conjugated phenylene group adjacent to the other side of $\mathbf{V}$ is virtually equal to distance $d_6$. This is probably also owing to the fact that the

Table 1. Effective distances [Å] between protons $H_{11}$ and $H_x$ in [2]rotaxane **8**·2PF$_6$ for experimental and model conformations.

| $H_x$ | No. $H_x$ protons | Conformations | | |
|---|---|---|---|---|
| | | Experimental[a] | Folded | Stretched |
| $H_1$ | 27 | $9.55 \pm 0.60$ | 9.22 | 12.22 |
| $H_2$ | 6 | $>8.80$[b] | 8.99 | 10.74 |
| $H_3$ | 6 | | 8.37 | 9.24 |
| $H_{25}$ | 2–6[c] | $6.44 \pm 0.33$ | 5.30 | 24.20 |
| $H_4$ | 2 | $5.58 \pm 0.20$ | 6.03 | 7.67 |
| $H_5$ | 2 | $4.41 \pm 0.09$ | 4.07 | 5.36 |
| $H_6$ | 2 | $4.35 \pm 0.08$ | 4.76 | 4.49 |
| $H_7$ | 2 | $3.86 \pm 0.05$ | 4.28 | 3.90 |
| $H_8$ | 2 | $3.85 \pm 0.05$ | 3.57 | 3.84 |
| $H_9$ | 2 | $4.31 \pm 0.08$ | 4.75 | 4.48 |
| $H_{10}$ | 8 | $3.20 \pm 0.03$ | 3.36 | 3.33 |
| $H_{15}$ | 2 | $>7.33$[b] | 5.85 | 5.99 |
| $H_{16}$ | 2 | $4.20 \pm 0.07$ | 4.62 | 6.17 |
| $H_{17}$ | 2 | $4.63 \pm 0.12$ | 5.30 | 8.25 |
| $H_{18}$ | 2 | $>7.33$[b] | 8.10 | 10.67 |
| $H_{19}$ | 2 | $>7.33$[b] | 8.79 | 12.23 |
| $H_{20}$ | 2 | $>7.33$[b] | 11.76 | 14.68 |
| $H_{21}$ | 2 | $>7.33$[b] | 12.85 | 16.02 |
| $H_{22}$ | 2 | $>7.33$[b] | 10.13 | 18.72 |
| $H_{23}$ | 2 | $>7.33$[b] | 8.92 | 21.12 |
| $H_{24}$ | 2–6[c] | $>7.54$[b] | 7.22 | 23.32 |
| $H_{26}$ | 9–27[c] | $7.59 \pm 0.83$ | 5.89 | 25.04 |

[a] Distances were calculated by using $d_{ref} = 3.20$ Å, based on X-ray data for the crystal structure of **10**·2PF$_6$. [b] No corresponding signal was observed in the NOE spectrum, the minimum distances (shown in italics) were estimated on the basis of the noise level in the spectrum and $d_{ref}$ (see above). [c] Ambiguity in the number of interacting protons corresponds to rotation of the $C_3$ symmetrical stopper $S_B$.

$p$-phenylene group is tilted with respect to the plane of the viologen.

Whereas the above analysis allowed localisation of the crown ether at **V**, the application of this approach to the remote flexible parts of **8**·2PF$_6$ was problematic. As a result of the sixth power decay of the NOE interactions with distance, these interactions are very sensitive to changes in the conformation of the flexible ether chain of the axle and the stoppers. Therefore, to assist the experimental NOE data, two hypothetical conformations of **8**·2PF$_6$ were modelled. They were termed folded and stretched on account of the conformation of the flexible chain of the axle. This approach allowed a comparative analysis of the effective distances $d_x$ obtained from experimental NOE spectrum and effective distances calculated for the two model structures to be conducted.

Rotaxane **8**$^{2+}$ (i.e., without counterions) was minimised in vacuum by using molecular mechanics routines (MacroModel 8.5 with AMBER force field) with two different constraints between two central quaternary carbon atoms of the stoppers, 19 and 33 Å. These minimisations produced the folded and stretched conformations shown in Figure 4.[19] The effective distances were then calculated by using Equation (1), which was applied to the distances in the model structures, for both of the minimised structures by assuming that the aromatic $H_{11}$ protons of **7** were irradiated. The results are presented in Table 1.

For certain proton sets whose signal could not be detected in the NOE spectrum, the minimum distances ($d_{min}$) were estimated according to Equation (2), which allowed comparisons between all of the conformations to be made. The noise level in the spectrum was substituted for NOE$_x$ in these cases as an upper limit for the NOE signal. Therefore, the $d_{min}$ values obtained (shown in italics) indicate that the $H_x$ protons in question do not, on average, approach the $H_{11}$ protons closer than $d_{min}$.

Comparison of the calculated distances (Table 1) shows that the folded conformation is a good approximation of the average structure of **8**·2PF$_6$ in solution. The results for the stopper ($S_B$) protons ($H_{25}$, $H_{26}$) are of particular relevance owing to the large differences between the two conformations for distances $d_{25}$ and $d_{26}$.

These results allow us to conclude that $S_B$ in **8**·2PF$_6$ folds back towards the centre of the molecule. The signals that correspond to protons $H_{25}$ and $H_{26}$ were observed in the NOE spectrum and a relatively good agreement was found between the experimental and calculated values of distances $d_{25}$ and $d_{26}$ in the folded conformation. The presence of a signal is itself an important observation because in the case
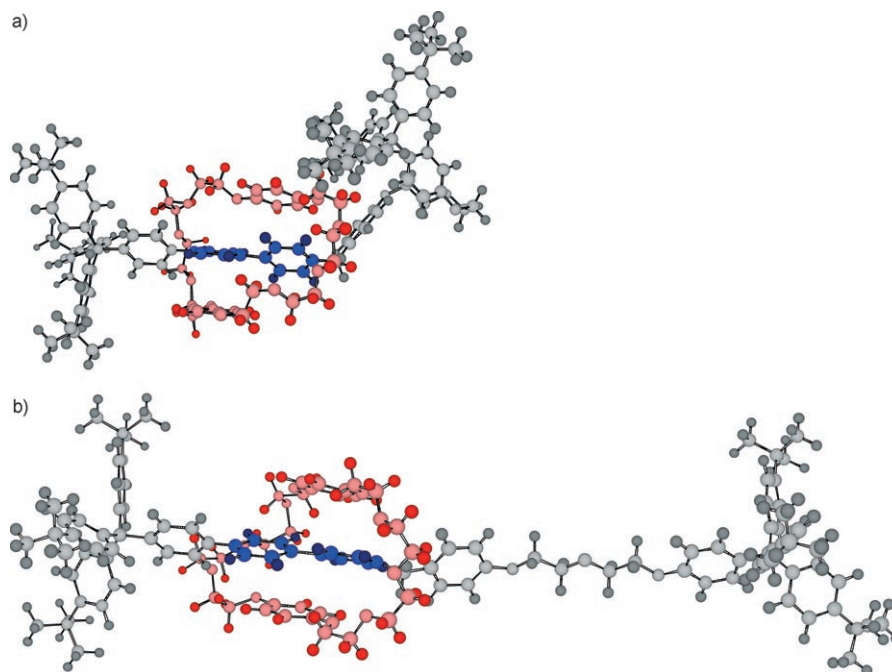


Figure 4. Model of the folded (top) and stretched (bottom) conformations of **8**·2PF$_6$.

of the stretched conformation protons $H_{25}$ and $H_{26}$ are far beyond the limit of the NOE interactions (24.20 and 25.04 Å, respectively).

The experimental values of $d_{25}$ and $d_{26}$ are in fact slightly greater than the corresponding values for the folded conformation, which suggests that, on average, rotaxane $8\cdot2PF_6$ adopts a more open conformation than that of the folded one in solution. It should be noted, however, that another effect may also contribute to the observed discrepancies. The calculated distances between the $S_B$ protons and the $H_{11}$ protons depend strongly on the internal conformation of $S_B$. Any changes to its conformation (including the orientation of the terminal *tert*-butyl groups) induce changes in the NOE interaction, and hence, in the calculated results. Therefore, the discrepancy in the $d_{26}$ values (8.12 vs. 5.89 Å) is still consistent with the folding of $S_B$ of the axle. For protons $H_{25}$ the analysis is more complicated because the signals of the $H_3$ and $H_{25}$ protons overlap. It is clear, nonetheless, that the experimentally determined distance for the combined set of $H_3$ and $H_{25}$ protons (6.64 Å) corresponds well to the values calculated separately for both sets in the folded conformation (8.37 and 5.30 Å, respectively), but not for the stretched conformation (9.24 and 24.20 Å).

No signal in the NOE spectrum was observed for the polyether flexible chain and the aromatic protons of the axle ($H_{18}$–$H_{22}$), which is in agreement with the distances calculated for both model conformations and the estimated detection limit. Whereas these interactions may not be used to discriminate between the folded and stretched conformations, the lack of corresponding signals in the spectrum provides an additional argument for the predominant localisation of **7** at the viologen station and against its shuttling along the axle.

The folded conformation exhibits a tilt of 66.8° of the *N*-benzyl aromatic ring with respect to the plane of viologen, which leads to the proximity of protons $H_{16}$ to the irradiated $H_{11}$ protons. The effective distance calculated for this conformation is comparable with the distance from the $H_9$ viologen protons to protons $H_{11}$. This result agrees well with the experimentally determined distance $d_{16}$, as discussed above.[20]

The analysis of the results obtained for the $H_1$ protons of stopper $S_A$ indicates that folded stopper $S_B$ provides a steric barrier to the movement of **7** along the axle of the rotaxane. This folding effectively locks the crown ether at the viologen. This conclusion is supported by very reasonable agreement between the experimental $d_1$ value (9.55 Å) and the distance $d_1$ calculated for the folded conformation (9.22 Å), whereas the experimental $d_1$ value is much shorter than that calculated for the stretched conformation (12.22 Å). In the stretched conformation the crown ether shifts towards the *N*-benzyl group because there is no steric barrier provided by stopper $S_B$.

A question arises about the reasons for the folding of the flexible axle chain and stopper $S_B$. It is possible that folding is driven by CH–π interactions between the *tert*-butyl groups of $S_B$ and the aromatic rings of the crown ether.[21]

**Structure of the radical cation of $8\cdot2PF_6$ in solution**: Many of the applications envisaged for redox-active [2]rotaxanes are based on assumptions about the relationship between the oxidation/reduction states of these molecules and their conformations in solution or at a surface.[1,7c,9] In this context, and having established the detailed conformation of $8\cdot2PF_6$ in solution, we have also investigated the detailed conformation in the singly reduced state when the interlocked molecule accepts an electron to form $8\cdot PF_6$.

The application of NMR spectroscopy to paramagnetic species is, generally speaking, problematic.[22–25] However, $^1H$ NMR spectroscopy has recently been used to structurally characterise the radical cation states of a series of viologens and [2]rotaxanes.[11,26] It was demonstrated that an analysis of spin relaxation paramagnetic enhancement can be used to reveal the position of the crown ether in [2]rotaxanes and to elucidate the conformation of the axle.[11]

Following a single-electron reduction of $8\cdot2PF_6$ by zinc in acetonitrile, the $^1H$ NMR spectrum of the corresponding radical cation was recorded at 25°C (Figure 2). It was found that in the NMR spectrum of $8\cdot PF_6$, all of the peaks belonging to the viologen moiety ($H_6$, $H_7$, $H_8$, $H_9$) and to adjacent positions ($H_{15}$, $H_{16}$, $H_{17}$, $H_5$, $H_4$, $H_3$) were no longer observed. The corresponding paramagnetic suppression zone (PSZ), surmised from these data, is represented in Figure 5 as a blue ellipsoid. However, the characteristic resonance of the aromatic protons of **7** at $\delta = 6.14$ ($H_{11}$) is observed in the NMR spectrum of $8\cdot PF_6$ and is not shifted.
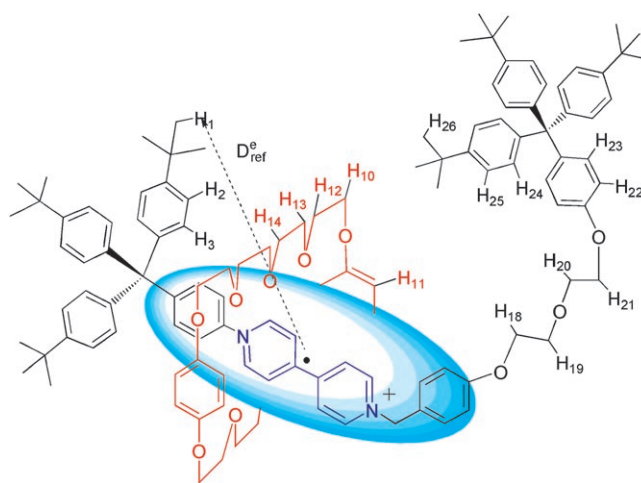


Figure 5. A possible representation of paramagnetic suppression zone in the [2]rotaxane $8\cdot PF_6$.

To determine the detailed conformation of $8\cdot PF_6$ in solution, the relaxation times ($T_1$) and relaxation rates ($R_1$) for all of the protons were measured as described in detail elsewhere.[11,23] Then, the values for electron–proton paramagnetic relaxation enhancement (PRE, $R_1^e$) were calculated on the basis of $T_1$ and $R_1$ for $8\cdot2PF_6$ and $8\cdot PF_6$ (Table 2).[11]

The values of $R_1^e$ do not provide, however, convenient means of analysing the conformation of $8\cdot PF_6$. They also do

Table 2. Relaxation times, rates and estimated effective distances in [2]rotaxane $8\cdot 2\,PF_6$.

| $H_x$ | Dication $T_1$ [s] | Dication $R_1$ [s$^{-1}$] | Radical cation $T_1$ [s] | Radical cation $R_1$ [s$^{-1}$] | PRE [s$^{-1}$] | $d_x^e$ | $d_x$ [f] |
|---|---|---|---|---|---|---|---|
| $H_1$ | 1.8 | 0.56 | 0.36 | 2.8 | 2 | 12.1±1.3 | 12.1 |
| $H_2$ | 1.35 | 0.74 | –[a] | –[b] | –[c] | <5.6[d,e] | 10.5 |
| $H_3$ | 1.2 | 0.81 | –[a] | –[b] | –[c] | <5.6[d,e] | 9.1 |
| $H_4$ | 0.94 | 1.1 | –[a] | –[b] | –[c] | <5.6[d,e] | 7.2 |
| $H_5$ | 0.94 | 1.1 | –[a] | –[b] | –[c] | <5.6[d] | 4.9 |
| $H_6$ | 0.87 | 1.15 | –[a] | –[b] | –[c] | <5.6[d] | 3.4 |
| $H_7$ | 0.87 | 1.15 | –[a] | –[b] | –[c] | <5.6[d] | 2.2 |
| $H_8$ | 0.87 | 1.15 | –[a] | –[b] | –[c] | <5.6[d] | 2.8 |
| $H_9$ | 0.87 | 1.15 | –[a] | –[b] | –[c] | <5.6[d] | 4.7 |
| $H_{10}$ | 0.43 | 2.3 | 0.0080 | 125 | 123 | 6.2±0.7 | 5.3 |
| $H_{11}$ | 1.1 | 0.93 | 0.0080 | 125 | 124 | 6.2±0.7 | 4.2 |
| $H_{12}$ | 0.43 | 2.3 | 0.0080 | 125 | 123 | 6.2±0.7 | 4.4 |
| $H_{13}$ | 0.43 | 2.3 | 0.0080 | 125 | 123 | 6.2±0.7 | 6.2 |
| $H_{14}$ | 0.43 | 2.3 | 0.080 | 12.5 | 10 | 9.4±1.0 | 7.0 |
| $H_{15}$ | 0.36 | 2.8 | –[a] | –[b] | –[c] | <5.6[d] | 6.3 |
| $H_{16}$ | 1.1 | 0.93 | –[a] | –[b] | –[c] | <5.6[d] | 6.4 |
| $H_{17}$ | 1.2 | 0.81 | –[a] | –[b] | –[c] | <5.6[d,e] | 8.2 |
| $H_{18}$ | 0.58 | 1.7 | 0.080 | 12.5 | 11 | 9.3±1.0 | 11.0 |
| $H_{19}$ | 0.65 | 1.5 | 0.22 | 4.5 | 3 | 11.5±1.4 | 11.1 |
| $H_{20}$ | 0.65 | 1.5 | 0.22 | 4.5 | 3 | 11.5±1.4 | 13.6 |
| $H_{21}$ | 0.58 | 1.7 | 0.22 | 4.5 | 3 | 11.6±1.5 | 14.6 |
| $H_{22}$ | 1.2 | 0.81 | 0.22 | 4.5 | 4 | 11.1±1.2 | 12.1 |
| $H_{23}$ | 1.2 | 0.81 | 0.29 | 3.5 | 3 | 11.7±1.3 | 11.4 |
| $H_{24}$ | 1.2 | 0.81 | 0.29 | 3.5 | 3 | 11.7±1.3 | 10.7 |
| $H_{25}$ | 1.2 | 0.81 | 0.22 | 4.5 | 4 | 11.1±1.2 | 9.7 |
| $H_{26}$ | 1.9 | 0.53 | 0.22 | 4.5 | 4 | 11.0±1.2 | 9.9 |

[a] $T_1$ is below $2.5\times10^{-3}$ s. [b] Expected $R_1$ is above $4.0\times10^2$ s$^{-1}$. [c] Very high PRE value. [d] Based on $R_1 > 4\times10^2$ s$^{-1}$ and by using Equation (4). [e] Discrepancy is caused by a high PRE owing to spin-diffusion within the aromatic system [f] Distances between the centre of the PSZ and $H_x$, in folded diastereomer (Figure 4a) by using Equation (1).

not allow a straightforward comparison with the structure of $8\cdot 2\,PF_6$, which was expressed in terms of effective distances, to be made. Therefore, the concept of effective distances was extended for PRE data. In this case, the effective distances were calculated between all $H_x$ proton groups and the centre of the PSZ (see Figure 5) arbitrarily located at the 4-position of the viologen pyridine ring adjacent to stopper $S_A$. This asymmetric location was chosen to account for the possible conjugation of $S_A$ with the viologen aromatic system and the respective delocalisation of the unpaired electron.

The effective distance from the centre of the PSZ to the $H_1$ protons for the folded conformation of $8\cdot 2\,PF_6$ was calculated by using Equation (1) and was used as $d_{ref}^e$ (Figure 5). The choice of the $H_1$ protons was based on the assumption that their position and respective distance do not change during reduction. The $d_x^e$ values between the centre of the PSZ and proton groups $H_x$ were then calculated by using Equation (4), which assumes a sixth power decay of $R_1^e$ with respect to the distance away from the centre of the PSZ. The results are given in Table 2. It is important to stress, however, that owing to delocalisation of the unpaired electron and strong spin diffusion in the vicinity of the viologen moiety, these results have to be treated carefully.

$$d_x^e = d_{ref}^e \left( \frac{PRE_{ref}}{PRE_x} \right)^{1/6} \qquad (4)$$

An analysis of the $d_x^e$ values, which were estimated from the PRE data, revealed that the ether chain of $S_B$ is folded in the reduced state of the [2]rotaxane ($8\cdot PF_6$). Specifically, the distances between the centre of the PSZ and protons $H_{25}$ and $H_{26}$ ($d^e = 11.11$ and $10.97$ Å, respectively) are in good agreement with the corresponding distances calculated for the folded conformation. It is concluded that the conformation of $S_B$ in $8\cdot PF_6$ in acetonitrile is similar to that of the parent dication form ($8\cdot 2\,PF_6$), that is, folded.

The distances between protons $H_{10}$ to $H_{13}$ in **7** and the centre of the PSZ are relatively short ($d_e \approx 6.2$ Å) and generally in agreement with the range of values expected for the model folded conformation and the crystal structure of $10\cdot 2\,PF_6$.[27]

It is, therefore, concluded that in $8\cdot PF_6$ the flexible polyether chain attached to $S_B$ remains in the folded conformation and that **7** remains localised at **V**. The latter is an important observation because there are three viable possibilities for the state of **7** after the reduction step: 1) it remains at **V**, 2) it travels without restraint along the axle or 3) it moves to the flexible polyether chain of the axle. The viability of the second option is based on a weakening of the electrostatic interaction between positively charged **V** and electron-rich **7** and a previously observed decomplexation of a [2]pseudorotaxane that contains a similar viologen moiety after single-electron reduction.[11] The third option is based on a possible affinity of **7** for polyether chain units.[28] The results presented herein indicate that the interactions of **7** with **V** remain relatively strong in the singly reduced state and underline the crucial role of the folding of the polyether chain of the axle, which locks **7** into position.

**Electrochemical study of the supramolecular function**: As the reduction potential of $8\cdot 2\,PF_6$ is the measure of how readily viologen accepts an electron, the value of the reduction potential is sensitive to the presence and the location of **7** in this [2]rotaxane. It has previously been demonstrated that the complexation of **7** with **V** shifts the reduction potential ($E$) of that moiety to more negative values.[5,10,14a] Therefore, the supramolecular electromechanical function of $8\cdot 2\,PF_6$ depends on the location of **7** and the ability of this [2]rotaxane to adopt various conformations in different oxidation states.

As shown above, the detailed conformational study of $8\cdot 2\,PF_6$ in its two oxidation states ($V^{2+}$ and $V^+$) reveals that the position of **7** and the conformation of $S_B$ remain very similar upon reduction. Because it is feasible to electrochemically study $8\cdot 2\,PF_6$ in various oxidation states, a comparative cyclic voltammetry study of $8\cdot 2\,PF_6$ and $9\cdot 2\,PF_6$ was undertaken.

CV measurements were carried out at a scan rate of $100\ mV\,s^{-1}$ by using a $0.1\ mol\,dm^{-3}$ solution of tetrabutylammonium perchlorate as an electrolyte and non-aqueous Ag/AgNO$_3$ as the reference electrode. The voltammograms re-

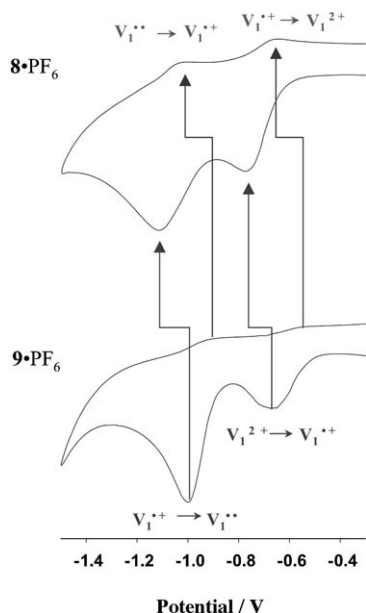corded are shown in Figure 6 and the respective peak potentials ($E_{peak}$) are given in Table 3.



Figure 6. Cyclic voltammograms of $8 \cdot 2PF_6$ ($3.0 \cdot 10^{-3}$ mol dm$^{-3}$) and $9 \cdot 2PF_6$ ($3.0 \cdot 10^{-3}$ mol dm$^{-3}$) were recorded at 100 mV s$^{-1}$ and 25 °C in acetonitrile containing TBAP (0.10 mol dm$^{-3}$).

Table 3. Cyclic voltammetry data[a] for [2]rotaxane $8 \cdot 2PF_6$ and the corresponding axle $9 \cdot 2PF_6$.[b]

|  | $E_{peak}$ $9 \cdot 2PF_6$ [mV] | $E_{peak}$ $8 \cdot 2PF_6$ [mV] | $\Delta E$ [mV] |
|---|---|---|---|
| $V^{2+} \rightarrow V^{+\cdot}$ | $-668 \pm 10$ | $-767 \pm 10$ | $-99 \pm 14$ |
| $V^{+\cdot} \rightarrow V^0$ | $-998 \pm 10$ | $-1107 \pm 10$ | $-109 \pm 14$ |

[a] Values correspond to first derivative zero crossing points. [b] At a concentration of $3.0 \times 10^{-3}$ mol dm$^{-3}$ in acetonitrile that contains the supporting electrolyte $n$Bu$_4$NClO$_4$ (0.010 mol dm$^{-3}$), scan rate 100 mV s$^{-1}$, 25 °C.

The negative shifts found for the two reduction and two oxidation peaks $E_{peak}$ in $8 \cdot 2PF_6$ mark a significant intercomponent interaction within $8 \cdot 2PF_6$ in its various oxidation states. More specifically, it can be concluded that in both oxidation states ($V^{2+}$ and $V^+$) 7 is localised on the viologen moiety. Interestingly, a negative shift in the first oxidation peak $V^0 \rightarrow V^+$ (Figure 6) shows that even in the fully reduced state of $V^0$, it is possible that 7 remains localised at the viologen moiety. These findings are in full agreement with the structural interpretation of the NOE, PASSY and the $T_1$ relaxometry measurements as well as with earlier reported findings for similar tripodal [2]rotaxanes on surfaces.[10]

## Conclusion

The methodology presented herein allowed us to characterise diastereoisomerism and conformations of the model rotaxane $8 \cdot 2PF_6$ in solution. It was demonstrated that 7 is localised at **V** in $8 \cdot 2PF_6$ and the flexible stopper group is folded back to the centre of the molecule. In the singly reduced state of $8 \cdot PF_6$, the position of 7 does not significantly change and the interaction with the viologen moiety is not completely inhibited. Additionally, the folding of $S_B$, which is possibly driven by CH–π interactions, provides further stabilisation of 7 at **V** in $8 \cdot PF_6$.

It can be concluded that the technique presented is a useful tool to study structure and conformations of interlocked systems in both diamagnetic and paramagnetic states. The conformational factors can significantly influence expected electrochemical and electromechanical function of interlocked molecules.

The reported methodology provides a level of insight that is arguably unnecessary to fully analyse the simple model [2]rotaxane $8 \cdot 2PF_6$. It was, nevertheless, presented in its entirety to demonstrate the capabilities of the methodology, but also to provide an important reference point for the study of switchable [2]rotaxanes in solution, and possibly, at the surface. In this context, the structural studies of more complex bistable [2]rotaxanes by using the above approach are reported in Part 2 of this paper.

## Experimental Section

NMR spectra were recorded by using a Varian Inova 300 or a Varian Inova 500 spectrometer in acetonitrile at 25 °C. For the PASSY measurements, solutions ($10^{-2}$ mol dm$^{-3}$) were deoxygenated in the NMR tube (Wilmad 535 PP-8 equipped with a rubber septum Z124338) by two successive freeze–pump–thaw cycles. Zinc filings (10 mg) were then added and the solutions deoxygenated by a further two successive freeze–pump–thaw cycles. Finally, the above samples were sonicated for 5 min under nitrogen and NMR spectra of the resulting deeply coloured solutions of the radical cation were recorded.

$T_1$ relaxation times were measured by using the inversion recovery method on a Varian Inova 500 spectrometer at 25 °C.[23,24] The samples were irradiated by using the following sequence, $D_1 = 8$ s and $P_1 = 180°$, $D_2$ in the range $10^{-5}$ to 2 s and $P_2 = 90°$.

Mass spectra were recorded by using a Finnigan Mat INCOS 50 quadrupole mass spectrometer. CVs were recorded by using a Solartron SI 1287 potentiostat controlled by a Labview program running on a Macintosh Power PC at a scan rate of 100 mV s$^{-1}$. All CVs were recorded under the following conditions: The working electrode was an isolated platinum wire. The counter electrode was an isolated platinum foil. The reference electrode was a non-aqueous Ag/Ag$^+$ electrode with a fill solution that consisted of AgNO$_3$ (0.010 mol dm$^{-3}$) in the electrolyte solution. The electrolyte solution consisted of tetrabutylammonium perchlorate (0.10 mol dm$^{-3}$) in dry solvent. All compounds were separately dissolved in the electrolyte solutions, which were bubbled with argon gas for 20 min prior to measurements being recorded.

Crystal data were collected by using a Bruker SMART APEX CCD area detector diffractometer. A full sphere of the reciprocal space was scanned by phi-omega scans. Pseudo-empirical absorption correction based on redundant reflections was performed by the program SADABS.[29a] The structure was solved by direct methods by using SHELXS-97 and refined by full-matrix least-squares on F2 for all data by using

SHELXL-97.[29b,c] Hydrogen atoms were added at calculated positions and refined by using a riding model. Their isotropic temperature factors were fixed to 1.2 times (1.5 times for methyl groups) the equivalent isotropic displacement parameters of the carbon atom to which the hydrogen atom is attached. Anisotropic temperature factors were used for all non-hydrogen atoms.

Melting points were estimated by using a Gallenkamp melting point device and were not corrected. Reagents and solvents were purchased from suppliers and used as received. All reactions were performed under nitrogen by using glassware that was flame dried. Chromatographic separations were performed by using silica (Merck, 40–63 micron) and the specified solvent system.

Compounds **2**,[15] **4·Cl**,[14] **6**[15] and **7**[30] were prepared by following previously reported procedures.

**Amine 3:** Alcohol **2** (0.23 g, 0.54 mmol) and aniline hydrochloride (0.14 g, 1.08 mmol) were heated in acetic acid (10 mL) at 110 °C in a sealed tube for 3 h. The solvent was evaporated under vacuum, after which methanol (15 mL) and HCl (2 mol dm$^{-3}$, 1 mL) were added. The slurry was stirred under reflux for 20 h and the solvent was evaporated under reduced pressure. The residue was extracted with chloroform and washed with aqueous NaHCO$_3$. The extract was dried over MgSO$_4$ and then was concentrated under reduced pressure. The residue was purified by column chromatography (ethyl acetate/cyclohexane) to give **3** as a pale solid (0.25 g, 93 %): M.p. 286 °C (lit. m.p. 288 °C[15a]); $^1$H NMR (CDCl$_3$, 300 MHz): $\delta = 7.22$ (d, $J = 8.8$ Hz, 6H), 7.08 (d, $J = 8.6$ Hz, 6H), 6.95 (d, $J = 8.6$ Hz, 2H), 6.56 (d, $J = 8.6$ Hz, 2H), 1.29 ppm (s, 27H); MS (ES): $m/z$: 504.2 [$M$+H]$^+$.

**Monocation 5·PF$_6$:** Amine **3** (0.1 g, 0.198 mmol) and the salt **4·Cl** (0.11 g, 0.3 mmol) were heated in dry ethanol (12 mL) at 80 °C in a sealed tube for 25 h. The solvent was evaporated under reduced pressure. The residue was dissolved in chloroform (60 mL) and was washed several times with water to remove excess reagent. The organic layer was dried over MgSO$_4$ and then was concentrated. The residue was purified by column chromatography (MeOH then MeOH/MeNO$_2$/KPF$_6$ (aq) 8.5:1:0.5). The respective fraction was concentrated under vacuum, the residue was dissolved in MeNO$_2$ and the organic phase was washed with water to remove excess of KPF$_6$. The solvent was evaporated under vacuum to give **5·PF$_6$** as a yellow solid (0.114 g, 73 %): Decomp 230 °C; $^1$H NMR (CD$_3$OD, 300 MHz): $\delta = 9.03$ (d, $J = 7$ Hz, 2H), 8.86 (d, $J = 6$ Hz, 2H), 8.48 (d, $J = 7$ Hz, 2H), 7.84 (d, $J = 6$ Hz, 2H), 7.60 (d, $J = 2.2$ Hz, 4H), 7.30 (d, $J = 8.6$ Hz, 6H), 7.12 (d, $J = 8.6$ Hz, 6H), 1.32 ppm (s, 27H); MS (ES): $m/z$: 643.2 [$M - $PF$_6$]$^+$; elemental analysis calcd (%) for C$_{47}$H$_{51}$N$_2$PF$_6$: C 71.56, H 6.52, N 3.55; found: C 71.00, H 6.53, N 3.52.

**[2]Rotaxane 8·2PF$_6$ and compound 9·2PF$_6$:** Monocation **5·PF$_6$** (36 mg, 0.045 mmol) and crown ether **7** (50 mg, 0.09 mmol) were added to **6** (50 mg, 0.065 mmol) in benzonitrile (0.2 mL) at room temperature. After 5 d the residue was purified by column chromatography (SiO$_2$; MeOH then MeOH/MeNO$_2$/KPF$_6$ (aq) 9.25:0.5:0.25 v/v) to give **9·2PF$_6$** as a yellow solid (26 mg, 37 %) and **8·2PF$_6$** as a red glassy solid (54 mg, 56 %).

**8·2PF$_6$:** $^1$H NMR (CD$_3$CN, 500 MHz): $\delta = 9.16$ (d, $J = 7.2$ Hz, 2H), 8.87 (d, $J = 6.9$ Hz, 2H), 8.00 (d, $J = 7.2$ Hz, 2H), 7.86 (d, $J = 6.9$ Hz, 2H), 7.78 (d, $J = 9$ Hz, 2H), 7.73 (d, $J = 9$ Hz, 2H), 7.66 (d, $J = 8.7$ Hz, 2H), 7.41 (d, $J = 8.7$ Hz, 6H), 7.30 (d, $J = 9.4$ Hz, 12H), 7.14 (d, $J = 8.7$ Hz, 8H), 7.10 (d, $J = 9.0$ Hz, 2H), 6.78 (d, $J = 9.0$ Hz, 2H) 6.14 (s, 8H), 5.86 (s, 2H), 4.20 (septuplet, $J = 4.7$ Hz, 2H), 4.07 (t, $J = 4.7$ Hz, 2H), 3.86 (t, $J = 4.7$ Hz, 2H), 3.82 (t, $J = 4.7$ Hz, 2H), 3.64–3.52 (m, 24H), 3.47–3.40 (m, 8H), 1.33 (s, 27H), 1.29 ppm (s, 27H); MS (ES) $m/z$: 931.1 [$M - 2$PF$_6$]$^{2+}$; elemental analysis calcd (%) for C$_{123}$H$_{148}$F$_{12}$N$_2$O$_{13}$P$_2$: C 68.63, H 6.93, N 1.30; found: C 68.21, H 6.95, N 1.50.

**9·2PF$_6$:** $^1$H NMR (CD$_3$CN, 500 MHz): $\delta = 9.11$ (d, $J = 6.9$ Hz, 2H), 8.98 (d, $J = 6.6$ Hz, 2H), 8.53 (d, $J = 6.7$ Hz, 2H), 8.44 (d, $J = 6.7$ Hz, 2H), 7.66–7.72 (m, 4H), 7.5 (d, $J = 8.9$ Hz, 2H), 7.41 (d, $J = 8.5$ Hz, 6H), 7.32 (d, $J = 8.6$ Hz, 6H), 7.25 (d, $J = 8.5$ Hz, 6H), 7.18–7.22 (m, 8H), 7.07 (d, $J = 8.8$ Hz, 2H), 6.83 (d, $J = 8.9$ Hz, 2H), 5.78 (s, 2H), 4.18 (t, $J = 4.5$ Hz, 2H), 4.10 (t, $J = 4.5$ Hz, 2H), 3.85–3.90 (m, 4H), 1.33 (s, 27H), 1.29 ppm (s, 27H); MS (ES): $m/z$: 1324.8 [$M - 2$PF$_6$]$^+$.

**[2]Pseudorotaxane 10·2PF$_6$:** 1,1′-diethyl-4,4′-bipyridinium bis(hexafluorophosphate) (0.005 g, 0.010 mmol) and **7** (0.0054 g, 0.010 mmol) were dissolved in acetone (0.5 mL) and the solution was concentrated by using vapour diffusion conditions to give **10·2PF$_6$** as a red solid (100 %). M.p. 121 °C (reversible decomposition into **V** and **7**); $^1$H NMR (CD$_3$CN, 300 MHz): $\delta = 9.35$ (d, $J = 7.0$ Hz, 2H), 8.59 (d, $J = 7.0$ Hz, 2H), 6.54 (s, 8H), 5.01 (q, $J = 7.5$ Hz, 4H), 3.82–3.84 (m, 8H), 3.71–3.75 (m, 8H), 3.72 (s, 16H), 1.83 ppm (t, $J = 7.5$ Hz, 6H); elemental analysis calcd (%) for C$_{42}$H$_{58}$F$_{12}$N$_2$O$_{10}$P$_2$: C 48.47, H 5.62, F 45.21, N 2.29; found: C 48.48, H 5.71, N 2.28.

Compound **10·2PF$_6$** was crystallised from acetone to obtain triclinic crystals of **10·2PF$_6$·2C$_3$H$_6$O** suitable for X-ray diffractometry measurements. CCDC-648423 contains the supplementary crystallographic data for this paper. These data can be obtained free of charge from The Cambridge Crystallographic Data Centre via www.ccdc.cam.ac.uk/data_request/cif.

[1] a) A. H. Flood, R. J. A. Ramirez, W. Deng, R. P. Muller, W. A. Goddard, J. F. Stoddart, *Aust. J. Chem.* **2004**, *57*, 301–322; b) P. M. Mendes, A. H. Flood, J. F. Stoddart, *Appl. Phys. A: Mater. Sci. Process.* **2005**, *80*, 1197–1209; c) J. W. Choi, A. H. Flood, D. W. Steuerman, S. Nygaard, A. B. Braunschweig, N. N. P. Moonen, B. W. Laursen, Y. Luo, E. DeIonno, A. J. Peters, J. O. Jeppesen, K. Yu, J. F. Stoddart, J. R. Heath, *Chem. Eur. J.* **2006**, *12*, 261–279.

[2] Following IUPAC nomenclature, the term diastereoisomer is used here to indicate any particular spatial arrangement of the atoms, diastereoisomers that can be interconverted by rotation about single bonds are referred to as conformations and translational isomers are referred to as co-conformations.

[3] a) M. C. T. Fyfe, P. T. Glink, S. Menzer, J. F. Stoddart, A. J. P. White, D. J. Williams, *Angew. Chem.* **1997**, *109*, 2158–2160; *Angew. Chem. Int. Ed. Engl.* **1997**, *36*, 2068–2070; b) J. F. Stoddart, S. A. Vignon, *Collect. Czech. Chem. Commun.* **2005**, *70*, 1493–1576.

[4] a) J. D. Badjic, V. Balzani, A. Credi, S. Silvi, J. F. Stoddart, *Science* **2004**, *303*, 1845–1849; b) P. R. Ashton, R. Ballardini, V. Balzani, I. Baxter, A. Credi, M. C. T. Fyfe, M. T. Gandolfi, M. Gomez-Lopez, M. V. Martinez-Diaz, A. Piersanti, N. Spencer, J. F. Stoddart, M. Venturi, A. J. P. White, D. J. Williams, *J. Am. Chem. Soc.* **1998**, *120*, 11932–11942.

[5] a) P. R. Ashton, R. Ballardini, V. Balzani, A Credi, K. R. Dress, E. Ishow, C. J. Kleverlaan, O. Kocian, J. A. Preece, N. Spencer, J. F. Stoddart, M. Venturi, S. Wenger, *Chem. Eur. J.* **2000**, *6*, 3558–3574; b) V. Balzani, M. Clemente-León, A. Credi, B. Ferrer, M. Venturi, A. H. Flood, J. F. Stoddart, *Proc. Natl. Acad. Sci. USA* **2006**, *103*, 1178–1183; c) C. P. Collier, E. W. Wong, M. Belohradsky, F. M. Raymo, J. F. Stoddart, P. J. Kuekes, R. S. Williams, J. R. Heath, *Science* **1999**, *285*, 391–394; d) C. P. Collier, G. Mattersteig, E. W. Wong, Y. Luo, K. Beverly, J. Sampaio, F. M. Raymo, J. F. Stoddart, J. R. Heath, *Science* **2000**, *289*, 1172–1175.

[6] a) G. Bottari, D. A. Leigh, E. M. Perez, *J. Am. Chem. Soc.* **2003**, *125*, 13360–13361; b) A. P. de Silva, N. D. McClenaghan, *Chem. Eur. J.* **2004**, *10*, 574–586; c) H. Azehara, W. Mizutani, Y. Suzuki, T. Ishida, Y. Nagawa, H. Tokumoto, K. Hiratani, *Langmuir* **2003**, *19*, 2115–2123; d) J. Berna, D. A. Leigh, M. Lubomska, S. M. Mendoza, E. M. Perez, P. Rudolf, G. Teobaldi, F. Zerbetto, *Nat. Mater.* **2005**, *4*, 704–710; e) H. Murakami, A. Kawabuchi, K. Kotoo, M. Kunitake, N. Nakashima, *J. Am. Chem. Soc.* **1997**, *119*, 7605–7606; f) C. A. Stanier, S. J. Alderman, T. D. W. Claridge, H. L. Anderson, *Angew.*

*Chem.* **2002**, *114*, 1847–1850; *Angew. Chem. Int. Ed.* **2002**, *41*, 1769–1772.

[7] a) M. C. Jimenez, C. Dietrich-Buchecker, J.-P. Sauvage, *Angew. Chem.* **2000**, *112*, 3422–3425; *Angew. Chem. Int. Ed.* **2000**, *39*, 3284–3287; b) V. Balzani, M. Gomez-Lopez, J. F. Stoddart, *Acc. Chem. Res.* **1998**, *31*, 405–414; c) T. Yamamoto, H.-R. Tseng, J. F. Stoddart, V. Balzani, A. Credi, F. Marchioni, M. Venturi, *Collect. Czech. Chem. Commun.* **2003**, *68*, 1488–1514; d) W. Q. Deng, R. P. Muller, W. A. Goddard, *J. Am. Chem. Soc.* **2004**, *126*, 13562–13563; e) D. A. Leigh, A. Troisi, F. Zerbetto, *Angew. Chem.* **2000**, *112*, 358–361; *Angew. Chem. Int. Ed.* **2000**, *39*, 350–353; f) J. V. Hernandez, E. R. Kay, D. A. Leigh, *Science* **2004**, *306*, 1532–1537; g) A. Godt, G. Jeschke, *Magn. Reson. Chem.* **2005**, 43, S110-S118; h) O. F. A. Larsen, P. Bodis, W. J. Buma, J. S. Hannam, D. A. Leigh, S. Woutersen, *Proc. Natl. Acad. Sci. USA* **2005**, *102*, 13378–13382.

[8] a) R. Bissel, E. Cordoba, A. E. Kaifer, J. F. Stoddart, *Nature* **1994**, *369*, 133–137; b) A. Livoreil, C. Dietrich-Buchecker, J.-P. Sauvage, *J. Am. Chem. Soc.* **1994**, *116*, 9399–9400.

[9] H.-R. Tseng, S. A. Vignon, P. S. Celestre, J. Perkins, J. O. Jeppesen, A. Di Fabio, R. Ballardini, M. T. Gandolfi, M. Venturi, V. Balzani, J. F. Stoddart, *Chem. Eur. J.* **2004**, *10*, 155–172.

[10] B. Long, K. Nikitin, D. Fitzmaurice, *J. Am. Chem. Soc.* **2003**, *125*, 15490–15498.

[11] a) K. Nikitin, D. Fitzmaurice, *J. Am. Chem. Soc.* **2005**, *127*, 8067–8076; b) K. Nikitin, E. Lestini, J. K. Stolarczyk, H. Müller-Bunz, D. Fitzmaurice, *Chem. Eur. J.* **2008**, *14*, 1117–1128.

[12] D. Neuhaus, M. P. Williamson, *The Nuclear Overhauser Effect in Structural and Conformational Analysis*, 2nd ed., Wiley-VCH, New York, **2000**.

[13] a) P. R. Ashton, R. Ballardini, V. Balzani, I. Baxter, A. Credi, M. C. T. Fyfe, M. T. Gandolfi, M. Gomez-Lopez, M. V. Martinez-Diaz, A. Piersanti, N. Spencer, J. F. Stoddart, M. Venturi, A. J. P. White, D. J. Williams, *J. Am. Chem. Soc.* **1998**, *120*, 11932–11942; b) A. C. Benniston, A. Harriman, V. Lynch, *J. Am. Chem. Soc.* **1995**, *117*, 5275–5291; c) C. A. Hunter, *J. Am. Chem. Soc.* **1992**, *114*, 5303–5311; d) P. R. Ashton, J. A. Bravo, F. M. Raymo, J. F. Stoddart, A. J. P. White, D. J. Williams, *Eur. J. Org. Chem.* **1999**, 899–908; e) A. B. Braunschweig, C. M. Ronconi, J.-Y. Han, F. Aricó, S. J. Cantrill, J. F. Stoddart, S. I. Khan, A. J. P. White, D. J. Williams, *Eur. J. Org. Chem.* **2006**, 1857–1866.

[14] a) B. Long, K. Nikitin, D. Fitzmaurice, *J. Am. Chem. Soc.* **2003**, *125*, 5152–5160; b) M. Hanke, C. Jutz, *Synthesis* **1980**, 31–32.

[15] a) H. W. Gibson, S.-H. Lee, P. T. Engen, P. Lecavalier, J. Sze, Y. X. Shen, M. Bheda, *J. Org. Chem.* **1993**, *58*, 3748–3756; b) P. R. Ashton, R. Ballardini, V. Balzani, M. Belohradsky, M. T. Gandolfi, D. Philp, L. Prodi, F. M. Raymo, M. V. Reddington, N. Spencer, J. F. Stoddart, M. Venturi, D. J. Williams, *J. Am. Chem. Soc.* **1996**, *118*, 4931–4951; c) K. Nikitin, B. Long, D. Fitzmaurice, *Chem. Commun.* **2003**, 282–283.

[16] G. Hilmersson, P. I. Arvidsson, Ö. Davidsson, M. Håkansson, *J. Am. Chem. Soc.* **1998**, *120*, 8143–8149.

[17] P. M. Iovine, G. Veglia, G. Furst, M. J. Therien, *J. Am. Chem. Soc.* **2001**, *123*, 5668–5679.

[18] The resonances assigned to the aliphatic crown ether protons of **8**·2PF$_6$ (H$_{10}$, H$_{12}$, H$_{13}$ and H$_{14}$) overlap, and as a consequence, only

the summed cross-peak volume integral NOE$_{sum}$ can be extracted from the spectrum. NOE$_{ref}$ is then calculated as a contribution of the H$_{10}$–H$_{11}$ interactions to the NOE$_{sum}$. Aromatic crown ether protons H$_{11}$ are much closer to protons H$_{10}$ than to protons H$_{12}$, H$_{13}$ and H$_{14}$ in all conformations of the crown ether. Consequently the contribution of protons H$_{10}$ dominates in the total signal. It was assumed, therefore, that the contribution of H$_{10}$ could be calculated from the solid state structure of the auxiliary pseudorotaxane **10**·2PF$_6$ by using Equation (3):

$$\text{NOE}_{\text{ref}} = \frac{\sum_i^{n_{11}} \sum_j^{n_{10}} d_{ij}^{-\frac{1}{6}}}{\sum_i^{n_{11}} \left( \sum_j^{n_{10}} d_{ij}^{-\frac{1}{6}} + \sum_j^{n_{12}} d_{ij}^{-\frac{1}{6}} + \sum_j^{j_{13}} d_{ij}^{-\frac{1}{6}} + \sum_j^{n_{14}} d_{ij}^{-\frac{1}{6}} \right)} \text{NOE}_{\text{sum}} \qquad (3)$$

in which n$_{12}$, n$_{13}$ and n$_{14}$ are the numbers of H$_{12}$, H$_{13}$ and H$_{14}$ protons, respectively. By using the X-ray data for **10**·2PF$_6$ it was found that NOE$_{ref}$ = 0.96NOE$_{sum}$, that is, indeed NOE$_{ref}$ is a dominant contribution to NOE$_{sum}$. It can be concluded that using X-ray data here does not affect the accuracy of the calculations.

[19] Remarkably, the minimisation without any distance constraints resulted is a strongly folded conformation of the axle.

[20] The absence of the signal in the NOE spectrum that corresponds to protons H$_{15}$ can be attributed to relatively short relaxation time $T_1$ of H$_{15}$ (0.36 s, see Table 2) compared to $T_1$ of irradiated protons H$_{11}$ (1.1 s).

[21] M. Nishio, M. Hirota, *Tetrahedron* **1989**, *45*, 7201–7245.

[22] *NMR of Paramagnetic Molecules* (Eds.: G. N. La Mar, Jr., W. Horrocks, R. H. Holm), Academic Press, New York, **1973**.

[23] R. L. Vold, J. S. Waugh, M. P. Klein, D. E. Phelps, *J. Chem. Phys.* **1968**, *48*, 3831–3832.

[24] G. I. Likhtenshtein, I. Adin, A. Novoselsky, A. Shames, I. Vaisbuch, R. Glaser, *Biophys. J.* **1999**, *77*, 443–453.

[25] R. Sharp, L. Lohr, J. Miller, *Prog. Nucl. Magn. Reson. Spectrosc.* **2001**, *38*, 115–158.

[26] W. S. Jeon, E. Kim, Y. H. Ko, I. H. Hwang, J. W. Lee, S.-Y. Kim, H.-J. Kim, K. Kim, *Angew. Chem.* **2005**, 117, 89–93; *Angew. Chem. Int. Ed.* **2005**, *44*, 87–91.

[27] The effective distances between a specified carbon atom in the centre of the PSZ and protons H$_{10}$–H$_{13}$ calculated for the crystal structure of **10**·2PF$_6$ are within the range of 4.03 to 7.48 Å.

[28] a) H. Kitano, T. Hirabayashi, M. Gemmei-Ide, M. Kyogoku, *Macromol. Chem. Phys.* **2004**, *205*, 1651–1659; b) Y. Kikuchi, Y. Aoyama, *Supramol. Chem.* **1996**, *7*, 147–152.

[29] a) G. M. Sheldrick, SADABS, Bruker AXS, Madison, WI 53711, **2000**; b) G. M. Sheldrick, SHELXS-97, Program for the Solution of Crystal Structures, University of Göttingen, Göttingen (Germany), **1997**; c) G. M. Sheldrick, SHELXL-97-2, Program for the Refinement of Crystal Structures, University of Göttingen, Göttingen (Germany), **1997**.

[30] a) R. C. Helgeson, T. L. Tarnowski, J. M. Timko, D. J. Cram, *J. Am. Chem. Soc.* **1977**, *99*, 6411; b) R. C. Helgeson, J. M. Timko, D. J. Cram, *J. Am. Chem. Soc.* **1974**, *96*, 7380.